EXPERIMENTAL LIMIT ON MONOJET PRODUCTION IN e^+e^--ANNIHILATION

CELLO Collaboration

H.-J. BEHREND, J. BÜRGER, L. CRIEGEE, H. FENNER, J.H. FIELD, G. FRANKE, J. FUSTER [1], Y. HOLLER, J. MEYER, V. SCHRÖDER, H. SINDT, U. TIMM, G.G. WINTER, W. ZIMMERMANN

Deutsches Elektronen-Synchrotron, DESY, D-2000 Hamburg 52, Germany

P.J. BUSSEY, A.J. CAMPBELL, J.B. DAINTON, D. HENDRY, G. McCURRACH, J.M. SCARR, I.O. SKILLICORN, K.M. SMITH

University of Glasgow, Glasgow G12 8QQ, United Kingdom

V. BLOBEL, M. POPPE, H. SPITZER

II. Institut für Experimentalphysik, Universität Hamburg, D-2000 Hamburg 50, Germany

W.-D. APEL, J. ENGLER, G. FLÜGGE, D.C. FRIES, W. FUES [2], K. GAMERDINGER, P. GROSSE-WIESMANN, J. HANSMEYER, Th. HENKES, G. HOPP, H. JUNG, J. KNAPP, M. KRÜGER, H. KÜSTER, H. MÜLLER, K.H. RANITZSCH, H. SCHNEIDER

Kernforschungszentrum Karlsruhe and Universität Karlsruhe, D-7500 Karlsruhe, Germany

W. DE BOER, G. BUSCHHORN, W. CHRISTIANSEN, G. GRINDHAMMER, B. GUNDERSON, Ch. KIESLING, R. KOTTHAUS, H. KROHA, D. LÜERS, H. OBERLACK, B. SACK, P. SCHACHT, G. SHOOSHTARI, W. WIEDENMANN

Max-Planck-Institut für Physik und Astrophysik, D-8000 Munich 40, Germany

A. CORDIER, M. DAVIER, D. FOURNIER, M. GAILLARD, J.F. GRIVAZ, J. HAISSINSKI, V. JOURNÉ, F. LE DIBERDER, E. ROS [3], A. SPADAFORA, J.-J. VEILLET

Laboratoire de l'Accélérateur Linéaire, F-91405 Orsay Cedex, France

B. FATAH, R. GEORGE, M. GOLDBERG, O. HAMON, F. KAPUSTA, F. KOVACS, R. PAIN, L. POGGIOLI, M. RIVOAL

Laboratoire de Physique Nucléaire et Hautes Energies, Université de Paris, F-75231 Paris Cedex 05, France

G. D'AGOSTINI, M. GASPERO, B. STELLA

University of Rome and INFN, I-00185 Rome, Italy

R. ALEKSAN, G. COZZIKA, Y. DUCROS, P. JARRY, Y. LAVAGNE, F. OULD SAADA, J. PAMELA, F. PIERRE, J. ZACEK [4]

Centre d'Etudes Nucléaires, Saclay, F-91191 Gif-sur-Yvette Cedex, France

G. ALEXANDER, G. BELLA, Y. GNAT and J. GRUNHAUS

Tel Aviv University, Ramat Aviv, Tel Aviv 69978, Israel

Received 9 July 1985

For footnotes see next page.

0370-2693/85/$ 03.30 © Elsevier Science Publishers B.V. (North-Holland Physics Publishing Division)

We have searched for monojet production in e^+e^--annihilation with the CELLO detector operating at the highest PETRA energies. No events were found, which makes it unlikely that the recently observed monojets in $p\bar{p}$ collisions originate from unusual Z^0 decays. The upper limits on monojet cross sections are compared with various models, thus yielding upper limits on the production cross sections of Higgs bosons and higgsinos.

Recently the UA1 Collaboration [1] reported the observation of a novel type of events in $p\bar{p}$ collisions, containing a single narrow jet of particles ("monojet") associated with a large missing transverse energy. They found no conventional explanation for such events within the standard model.

Many speculations about the origin of these events have been put forward. They can be grouped into two categories: (i) the monojets originate from new types of particles (e.g. composite, coloured or supersymmetric particles), or (ii) the monojets arise from unusual decays of neutral vector bosons (Z^0). The latter hypothesis has been put forward by Glashow and Manohar [2], who pointed out that in such a case, the monojets should also be observable in e^+e^--annihilation. With a branching ratio of Z^0 into monojets of a few percent as suggested by the $p\bar{p}$ data, the monojet production cross section is in the order of 0.5 pb at a center of mass energy of 44 GeV. Around this energy we have an integrated luminosity of about 22 pb^{-1}. Therefore, such a clean signature as a monojet should be observable.

In this letter we report on a search for monojets with the CELLO detector at PETRA. The CELLO detector is especially well suited for such a search, because it has an almost hermetic coverage for charged and neutral particle detection [3].

The data sample was taken in 3 runs with the following integrated luminosities:

11.5 pb^{-1} equally distributed between $\sqrt{s}$ = 40 and 46.78 GeV,
9.4 pb^{-1} at $\sqrt{s}$ = 44.0 GeV,
1.1 pb^{-1} at $\sqrt{s}$ = 46.3 GeV.

We briefly summarize the detector elements used in this analysis.

(a) The central tracking detector measures charged particles with $|\cos\theta| < 0.9$, where θ is the polar angle between the particles and the positron beam direction.

(b) 4 endcap proportional chambers, two on each side of the central detector, supplement the central detector for charge particle tracking in the range $0.90 < \cos\theta < 0.99$.

(c) The central calorimeter covers $|\cos\theta| < 0.86$. It consists of 20 radiation lengths of lead strips immersed in liquid argon. The showers are sampled 6 times in depth and the fine segmentation results in an angular resolution $\sigma_\varphi = (6 \pm 1)$ mrad in azimuth and $\sigma_\theta = (10 \pm 2)$ mrad in θ and an energy resolution of $\sigma_E/E = 0.05 + 0.10/\sqrt{E}$, where E is the shower energy in GeV.

(d) The endcap calorimeter covers $0.92 < |\cos\theta| < 0.99$, and is a lead–liquid-argon calorimeter with similar properties as the central calorimeter.

(e) A lead scintillator calorimeter covers $0.85 < |\cos\theta| < 0.93$. This so-called hole tagger covers the acceptance gap between the endcap and central calorimeter. Particles entering this region traverse 2 lead scintillator sandwiches with a total of about 8 radiation lengths of material before the final scintillator plane. A total of 16 modules are arranged such that 8 modules cover the complete azimuth on each side.

The trigger of interest for this search required at least 2 GeV deposited energy in the central liquid-argon calorimeter and at least one charged particle with a momentum of ~650 MeV/c transverse to the beam direction in the central tracking detector as found by a fast hardware processor. After processing all the events through the standard CELLO reconstruction programs, the following criteria were used for a preselection:

(1) A total energy of at least 2 GeV in the central liquid argon calorimeter.

(2) At least 1 track in the central detector coming from the interaction point with a transverse momentum $p_t > 400$ MeV/c, one additional track with $p_t > 120$ MeV/c, and a total energy of the charged tracks $> 0.05\sqrt{s}$. Here $\sqrt{s}$ is the center of mass energy.

[1] On leave of absence from Instituo de Fisica Corpuscular, Universidad de Valencia, Valencia, Spain.
[2] Present address: SCS, D-2000 Hamburg, Germany.
[3] Present address: Universidad Autónoma de Madrid, Canto Blanco, Madrid 34, Spain.
[4] On leave of absence from Nuclear Center, Charles University, CS-180 00 Prague 8, Czechoslovakia.

(3) A missing transverse momentum p_t of all charged and neutral particles exceeding $0.15\sqrt{s}$.

Monojets were selected by the following procedure:

(1) All particle momenta were projected onto the plane perpendicular to the beam axis ($r\phi$ projection).

(2) Each event was then divided into two half planes in the $r\phi$ projection by a plane through the interaction point and normal to the sphericity axis of the projected momenta.

(3) Monojets were defined as events having one hemisphere without charged particles and with an electromagnetic energy below 0.5 GeV.

The projection onto the $r\phi$-plane was made to eliminate the background from events with a strong boost along the beam direction, which originate either from initial state radiation with the photon escaping along the beampipe or from the collision of two virtual photons with one or both initial particles escaping along the beampipe. Such events tend to have all particles in one hemisphere, but in the $r\phi$-projection the two-jet structure is recovered, since p_t is approximately balanced if the undetected particles are confined to the beampipe region. The projection onto the $r\phi$-plane and the large missing momentum required in this plane make the background from multihadrons coming from e^+e^- annihilation with

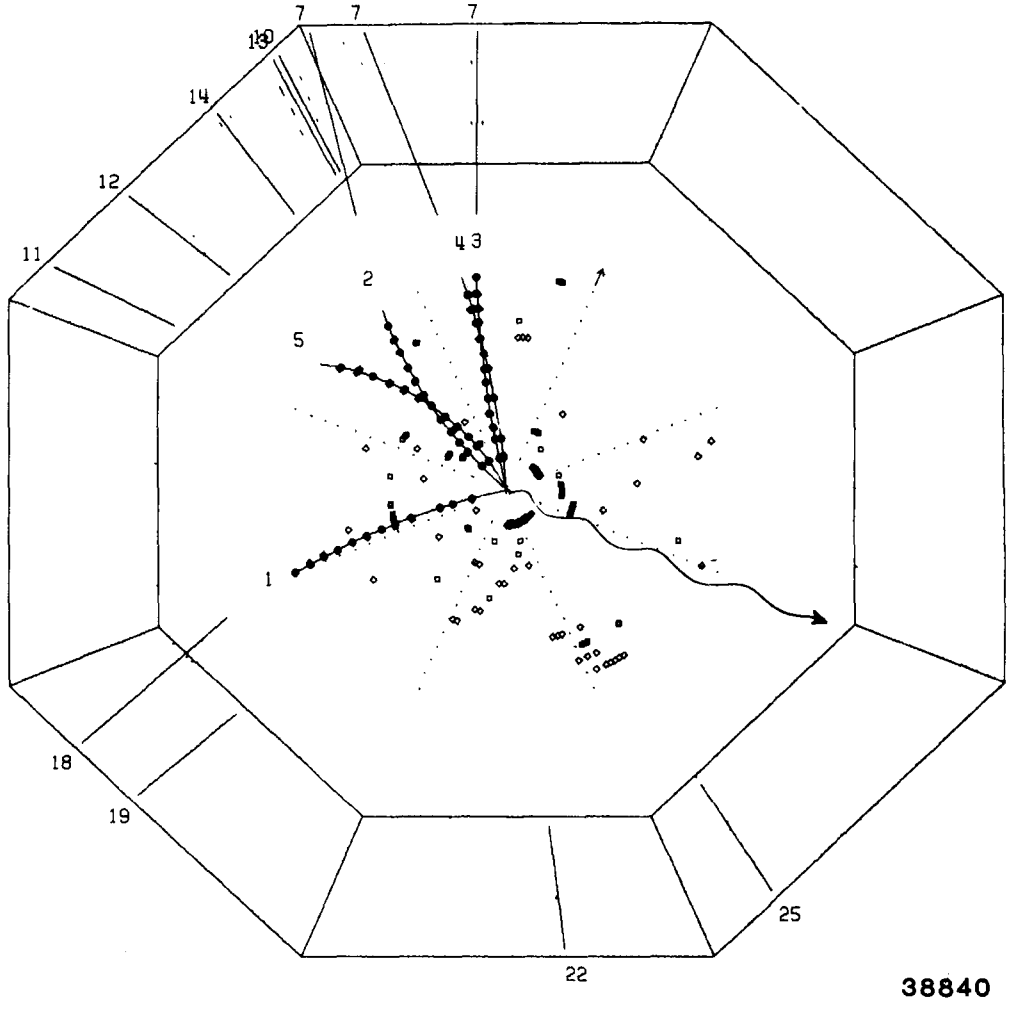

Fig. 1. An example of a monojet candidate. The event was rejected because of a photon (wiggled line) in the hole tagger.

initial state radiation and from two-photon collisions negligible as was determined from a Monte Carlo simulation. A non-negligible background source comes from $\tau\bar{\tau}$ pairs, of which one tau decays into a jet and the other one decays into one or two neutrinos and a charged particle which is either so soft that it stays inside the beampipe region or it escapes in the forward direction or it travels opposite to the parent tau direction. For our data sample we expect a total of 1.3 events from this source.

During the first part of the data (11.5 pb^{-1}) the hole tagger was not completely installed and monojet candidates from radiative Bhabha events were removed by requiring that for low multiplicities ($\leqslant 3$) no identified electrons were observed. An electron was identified by its shower in the liquid argon calorimeter. After this cut a total of 9 monojet candidates remained. After scanning them on an interactive graphic display, they were all rejected either because they originated from beam–gas interactions as was apparent from tracks not pointing to the interaction point (4 events), or they were rejected because of charged tracks in the "empty" hemisphere which were not found by the reconstruction programs (3 events), or they had a clear signal in the hole tagger (2 events). An example of such a monojet candidate with a signal in the hole tagger is shown in fig. 1.

Since no genuine monojets were observed, we can obtain an upper limit on the monojet cross section:

$$\sigma(e^+e^- \to Z^0_{\text{virtual}} \to X_1 + X_2) = N/\epsilon L$$

$$= \frac{G_F M_{Z^0} \Gamma_{Z^0} s[(1-4X)^2+1]}{2\sqrt{2}[(s-M^2_{Z^0})^2 + M^2_{Z^0}\Gamma^2_{Z^0}]}$$

$$\times \text{Br}(Z^0 \to X_1 + X_2)\lambda^{3/2}(1, m^2_{X_1}/s, m^2_{X_2}/s). \quad (1)$$

Here X_1 and X_2 are two new hypothetical scalar particles of which X_1 is assumed to be massless and to escape the detector without interactions and X_2 is assumed to decay hadronically. $G_F = 1.166 \times 10^{-5}$ GeV^{-2}, $M_{Z^0} = 93$ GeV, $\Gamma_{Z^0} = 3$ GeV, $X = \sin^2\theta_w = 0.214$, Br $(Z^0 \to X_1 + X_2)$ is the branching ratio for Z^0 into $X_1 + X_2$, assuming X_1 and X_2 to be massless and $\lambda(a, b, c) = a^2 + b^2 + c^2 - 2ab - 2bc - 2ac$ is a phase space factor taking the mass dependence into account for the available center of mass energy. L is our integrated luminosity. $N = 3$ is the 95% confidence level upper limit on the number of monojets, and ϵ is the efficiency to detect monojets with the cuts described above.

The efficiency has been determined with a complete Monte Carlo simulation of our detector using the Lund string fragmentation scheme [4] [‡1] and taking the radiative corrections to the virtual Z^0 exchange into account. We first make the simple assumption that X_2 has the same coupling to all quark pairs. Hereafter we will consider models with different couplings. The efficiency is 0.75 at $m_{X_2} = 5$ GeV, if we assume X_1 to decay promptly, so all decay products come from the interaction point. For lifetimes well above 10^{-11} s the efficiency will start to deteriorate. At higher masses the efficiency drops slowly because of the smaller Lorentz boost, which causes the jets to become broader and have particles in the hemisphere required to be empty. At $m_{X_1} = 15$ (20) GeV the efficiency has dropped to 0.43 (0.14). For masses below charm threshold the efficiency drops, because the fragmentation at such a low mass yields low multiplicities and sometimes only charged or only neutral particles, thus reducing the trigger efficiency. At $m_{X_2} = 2$ (1) GeV the efficiency is 0.54 (0.43). It should be noted that for low masses

[‡1] We used the updated version JETSET 5.2.

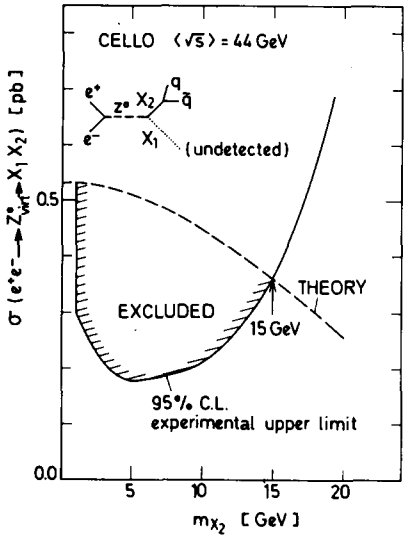

Fig. 2. The monojet cross section as function of the mass of the heaviest of the two hypothetical particles X_1 and X_2. X_1 is assumed to be massless and escapes the detector without interactions and X_2 is assumed to fragment randomly into the kinematically allowed $q\bar{q}$ pairs. The dashed curve was calcuated from eq. (1) with Br$(Z^0 \to X_1 + X_2) = 3\%$.

m_{X_2} the efficiency calculation becomes somewhat model dependent since the fragmentation models which are intended to fragment quarks at centre of mass energies where jets are observable (>7 GeV) do not take into account all dynamical effects which are expected to take place in the formation of resonances. Therefore m_{X_2} masses below 1 GeV were not considered.

Fig. 2 shows the 95% CL upper limit on the monojet cross section and the branching ratio of Z^0 into monojets using the efficiencies described above. For masses m_{X_2} below 15 GeV the 95% confidence level upper limit is below the monojet cross section expected for a branching ratio of 3%, which is the order of magnitude for the monojets observed at the $p\bar{p}$ collider.

In terms of the specific model of ref. [2] the monojets arise from the decay of Z^0 into 2 neutral Higgs bosons, h_1 and h_2. The branching ratio of Z^0 into h_1 and h_2 is $0.03\,\lambda^{3/2}\xi$. The factor ξ measures the mixing in the neutral boson sector [5] and is assumed to be close to its maximum value of 1. The mass of the scalar particle h_1 is supposed to be low, so that it has a long lifetime and it escapes from the detector before it decays. The pseudoscalar particle h_2 decays into quark and lepton pairs ($q\bar{q}$ and $\ell\bar{\ell}$) with branching ratios proportional to $3\,m_q^2\beta$ and $m_\ell^2\beta$ [‡2]. Here β is the fermion velocity and we take the current quark masses m_q of the u, d, s, c and b quarks to be 0.0, 0.0, 0.15, 1.6 and 5 GeV, respectively. We neglected three-body decay modes, which are likely to be small [2]. As shown in fig. 3, the experimental 95% CL upper limit on the cross section is below the theoretical cross section for masses between 1.2 and 13.6 GeV, thus excluding h_2 masses in this range. The limit on the cross section at low and high masses is somewhat less stringent in fig. 3 than in fig. 2 because at Higgs masses below 4 GeV h_2 fragments mainly into strange quarks. This leads to a larger fraction of purely neutral kaon final states, thus reducing the trigger efficiency. At high masses the limit becomes worse because h_2 fragments mainly into bottom mesons which lead to broader jets and are thus less likely to be selected as monojets.

Higgs masses well above $b\bar{b}$ threshold (~10 GeV)

[‡2] For a pseudoscalar the decay rate is proportional to β as opposed to β^3 for a scalar – see ref. [6].

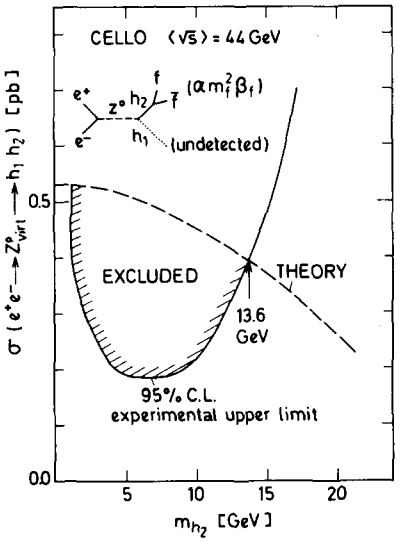

Fig. 3. As in fig. 2 with X_1 and X_2 replaced by neutral Higgs bosons.

give an averaged charged multiplicity above 7. This seems too high to explain the UA1 monojets, for which the observed charged multiplicity is less than 5 and the charged particle invariant mass is also small (<3.1 GeV).

A similar calculation can be performed if the neutral Higgs bosons are replaced by their supersymmetric counterparts, the higgsinos, denoted by χ_1 and χ_2. The mass of χ_1 is assumed to be 0, so that it will be stable and escape the detector without interactions. χ_2 is assumed to decay into χ_1 plus a $q\bar{q}$ pair via virtual Z^0-exchange, for which we used the matrix element given in ref. [7]. The direct two-body decay of χ_2 is forbidden, if we assume that the supersymmetric particles have their own conserved quantum number. In the limit of massless spin 1/2 higgsinos and assuming no mixing with the supersymmetric partners of the photon and Z^0 but a maximum mixing between the higgsinos, the total cross section is four times bigger than the corresponding cross section for Higgs bosons production [7] and the differential cross section is proportional to $1 + \cos^2\theta$ instead of $\sin^2\theta$. The hadronic final states are determined by the coupling of quarks to the Z^0 and the available phase space, which leads to a hadronic branching ratio of 50–70% for χ_2 masses between 2 and 20 GeV. The theoretical higgsino cross section is above the experimental 95% CL upper limit for χ_2

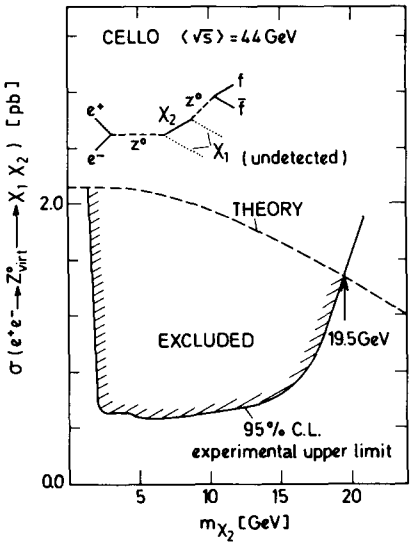

Fig. 4. As in fig. 2 with X_1 and X_2 replaced by neutral higgsinos. At low values of m_{X_2} this cross section is four times larger than in figs. 2 and 3 for the mixing conditions described in the text.

masses between 1.5 and 19.5 GeV (see fig. 4), thus excluding χ_2 masses in this range.

In conclusion, the non-observation of monojets in e^+e^- annihilation makes it unlikely that the monojets observed in $p\bar{p}$ collisions originate from unusual Z^0 decays. Similar conclusions have been reached by other collaborations [8].

We gratefully acknowledge the efforts of the PETRA machine group and the DESY computer center. The visiting groups wish to thank the DESY directorate for the hospitality experienced at DESY. Special thanks go to Dr. K. Hagiwara, Dr. W. Hollik, Dr. F. Schrempp, and Dr. B. Schrempp for helpful discussions.

References

[1] UA1 Collab., G. Arnison et al., Phys. Lett. 139B (1984) 115.
[2] S.L. Glashow and A. Manohar, Phys. Rev. Lett. 54 (1985) 526.
[3] CELLO Collab., H.-J. Behrend et al., Phys. Scr. 23 (1981) 610.
[4] T. Sjöstrand, Comput. Phys. Commun. 27 (1982) 243; 28 (1983) 229.
[5] G. Pocsik and G. Zsigmond, Z. Phys. C10 (1981) 367; N.G. Deshpande, X. Tata and D.A. Dicus, Phys. Rev. D29 (1984) 1527.
[6] F.M. Renard, Basics of electron positron collisions (Editions Frontières, Dreux, 1981).
[7] H. Baer, K. Hagiwara and S. Komamiya, Phys. Lett. 156B (1985) 117.
[8] HRS Collab., C. Akerlof et al., Phys. Lett. 156B (1985) 271;
JADE Collab., W. Bartel et al., Phys. Lett. 155B (1985) 288;
MAC Collab., W.W. Ash et al., Phys. Rev. Lett. 54 (1985) 2477;
MARK II Collab., G. Feldman et al., Phys. Rev. Lett. 54 (1985) 2289.